Accepted Manuscript

Authors: Lais C.G.F. Palhares, Adriana S. Brito, Marcelo A. de Lima, Helena B. Nader, James A. London, Igor L. Barsukov, Giulianna P.V. Andrade, Edwin A. Yates, Suely F. Chavante

A Further Unique Chondroitin Sulfate from the shrimp *Litopenaeus vannamei* with Antithrombin Activity that Modulates Acute Inflammation

Running title: Effect of Shrimp Chondroitin Sulfate on Inflammation

Lais C. G. F. Palhares[1,5], Adriana S. Brito[1,2], Marcelo A. de Lima[3,4], Helena B. Nader[3], James A. London[5], Igor L. Barsukov[5], Giulianna P. V. Andrade[1], Edwin A. Yates[5**], Suely F. Chavante [1*]

[1] *Programa de Pós-graduação em Bioquímica e Biologia Molecular, Departamento de Bioquímica, Universidade Federal do Rio Grande do Norte, Natal, RN, Brazil*

[2] *Faculdade de Ciências da Saúde do Trairi, Universidade Federal do Rio Grande do Norte, Santa Cruz, RN, Brazil*

[3] *Molecular & Structural Biosciences, School of Life Sciences, Keele University, Huxley Building, Keele, Staffordshire, ST5 5BG, United Kingdom*

[4] *Departamento de Bioquímica, Universidade Federal de São Paulo, SP, Brazil*

[5] *Department of Biochemistry, Institute of Integrative Biology, University of Liverpool, Liverpool, United Kingdom*

Corresponding authors: *Dra. Suely Ferreira Chavante, Departamento de Bioquímica, Universidade Federal do Rio Grande do Norte, Natal, RN, Brazil.Tel.: +55 8432153416 E-mail: suelychavante@gmail.com and **Dr. Edwin A. Yates, Department of Biochemistry, Institute of Integrative Biology, University of Liverpool, Liverpool, United Kingdom. E-mail: eayates@liverpool.ac.uk

Highlights

- A further shrimp chondroitin sulfate (sCS) was structurally characterized;
- sCS presents the rare 3-*O*-Sulfo-glucuronic acid residue;
- sCS inhibits thrombin and modulates *in vivo* inflammation

Abstract

The detailed structure of a further Chondroitin Sulfate from *Litopenaeus vannamei* shrimp (sCS) is described. The backbone structure was established by ^{1}H/^{13}C NMR, which identified 3-*O*-sulfated GlcA, 4-*O*-sulfated GalNAc, 6-*O*-sulfated GalNAc, and 4,6-di-*O*-sulfated GalNAc residues. GlcA is linked to GalNAc 4,6 di S and GlcA 3S is linked to GalNAc 4S, GalNAc 4,6 di-S and GalNAc6S residues. The anticoagulant properties of this sCS were evaluated by activated partial thromboplastin time, anti-IIa, anti-Xa and anti-heparin cofactor II-mediated activities, and sCS failed to stabilise antithrombin in a fluoresence shift assay. The anti-inflammatory effect of sCS was explored using a model of acute peritonitis, followed by leukocyte count and measurement of the cytokines, IL-1β, IL-6 and TNF-α. The compound showed low clotting effects, but high anti-IIa activity and HCII-mediated thrombin inhibition. Its anti-inflammatory effect was shown by leukocyte recruitment inhibition and a decrease in pro-inflammatory cytokine levels. Although the biological role of sCS remains unknown, its properties indicate that it is suitable for studies of multi-potent molecules obtained from natural sources.

Introduction

Chondroitin sulfate (CS) is a sulfated linear polysaccharide of the glycosaminoglycan (GAG) family, composed of β(1-4) linked disaccharide units, themselves comprising β-D-glucuronic acid (GlcA) (1→3) linked to N-acetyl-D-galactosamine (GalNAc) (Prabhakar & Sasisekharan, 2006; Tomatsu et al., 2015). Several types of CS structures have been reported and have been classified according to their GlcA and GalNAc sulfation patterns. Under this system of nomenclature, GalNAc residues sulfated at the C-4 and/or C-6 positions give rise to CS-A [GlcA-GalNAc 4-O-sulfate], CS-C [GlcA-GalNAc 6-O-sulfate] and CS-E [GlcA–GalNAc 4,6-di-O-sulfate] units respectively. GlcA residues exhibit *O*-sulfation at C-2 and more rarely at C-3, giving rise to CS-D [GlcA 2-O-sulfate-GalNAc 6-O-sulfate], CS-K [GlcA 3-O-sulfate-GalNAc 4-O-sulfate] and CS-S [GlcA 2,3 di-O-sulfate-GalNAc 4 or 6-O-sulfate] units, respectively (Cavalcante et. al., 2018; Nandini & Sugahara, 2006; Pavão, Vilela-Silva & Mourão 2006; Volpi 2006). Furthermore, sulfated fucose branches in GlcA residues are common in natural CS (Kale et al., 2013; Mou et al., 2018). It should be stressed, however, that CS polysaccharides isolated from invertebrates are rarely so well-defined; different sections of the CS chains often correspond to several of these supposed prototypical CS types. Recently, CS polysaccharides have attracted attention due to their participation in various biological events. Thus, the search for naturally occurring, novel CS (Deepa et. al. 2007; Shetty et.al. 2009; Toida et. al. 2015) has expanded, along with investigations into the relationship between their structural features and biological functions.

Sulfated GAGs are covalently bound to proteins to form several proteoglycans (PGs) that participate in numerous physiological phenomena. (Iozzo & Schaefer 2015; Ustyuzhanina et. al., 2018; Volpi, 2011). The variety in the position and degree of sulfation, size, number and disaccharide sequences that are inserted in the CSPGs, make CS a heterogeneous molecules. The many biological effects of CS so far reported include inflammation, cell proliferation, differentiation, migration, tissue morphogenesis and wound repair (Krichen et. al., 2018; Mou et. al. 2018; Sugahara et

al., 2003). Crucially, differences in the structure of CS chains lead to distinct biological and pharmacological properties.

Of all natural sources, marine GAGs stand out because of their structural peculiarities (Pomin & Morão, 2014). Recently, we characterized a CS from *Litopenaeus vannamei* shrimp (sCS) containing unusual 2,3-di-*O*-sulfated GlcA residues, which presented promising anticoagulant and antithrombotic activities (Cavalcante et. al., 2018). In addition, fucosylated CS structures obtained from distinct species of sea cucumber have been reported (Mou et. al., 2018; Ustyuzhanina et al., 2016). One major difference between these resides in the sulfation patterns of the fucose branches, which significantly affect their *in vitro* antioxidant properties. Even though CS structures have been isolated from many vertebrate and invertebrate animal species, (Krishen et; al., 2018; Shetty et. al., 2009; Sugahara et.al., 1996; Volpi & Maccari, 2007; Zhu et. al., 2018) the structural characterization of CS from invertebrate specimens reveals a rather narrow range of structures compared to those of marine species.

Here, a further sCS from *Litopenaeus vannamei* shrimp, isolated under different conditions and structurally distinct from that reported earlier (Cavalcante et al., 2018), which possesses inhibitory effects on inflammation and potent anti-thrombin activity, is structurally characterized.

Materials and methods

1. Cell culture and reagents

Murine macrophage cells (RAW 264.7) were grown in Dulbecco´s modified Eagle medium with 4.5 g.L^{-1} glucose supplemented with 10% fetal bovine serum and 20 mM sodium bicarbonate (Cultilab, Campinas, SP, Brazil). All cultures were performed in culture plates (Falcon BD, San Jose, CA, USA). Unfractionated Sodium heparin from porcine mucosa was obtained from Laboratory Derivati Organici (Trino Vercellese, Italy). Other reagents were purchased from Sigma (St Louis, MO, USA).

2. Animals

14 week old male Wistar rats weighing between 300 and 400 g and 12 week old female C57BL/6 mice (Departament of Biochemistry – Federal University of Rio Grande do Norte, Natal, Brazil) were used for *in vivo* experiments. Animals were housed in cages with free access to food and water and treated according to the ethical principles for animal experimentation. This study was carried out in strict accordance with the National Council on Animal Experimentation Control and specifically approved by the University of Rio Grande do Norte Ethics Committee.

3. Extraction of glycosaminoglycans and purification of a sCS from *L. vannamei*

The extraction procedure for shrimp GAGs was performed as previously described (Brito et. al., 2008; 2014). Heads of *Litopenaeus vannamei* shrimp were obtained from shrimps cultivated *in vivarium*, kindly provided by ENSEG Indústria Alimentícia LTDA, Macaíba, Brazil. Briefly, the shrimp heads were submitted to proteolysis and acetone treatment. The pool of GAGs obtained was fractionated using increasing volumes of acetone to obtain F-0.5A, F-0.7A and F-1.0A fractions. The sCS was then purified from F-1.0A, by further ion-exchange chromatography on DEAE-Sephacel, followed by NaCl elution (see Supplementary Data Fig. S1A and agarose electrophoresis profile in Fig.S1B). The sCS compound evaluated in this present study was eluted with 1.0M NaCl and is a distinct population of sCS isolated from fraction F-0,7A, previously reported (Cavalcante et al., 2018). Finally, the compounds were desalted by gel filtration through a Sephadex G-25 column by eluting with 10% ethanol. After lyophilization, this sCS sample was submitted to further analyses.

4. Molecular weight determination

The molecular weight (MW) of sCS was determined by gel permeation chromatography on a high-pressure liquid chromatography (GPC-HPLC) system, using a 300×7.8 mm BioSep SEC™ S-2000 LC column (Phenomenex, Torrance, CA, USA). Twenty μL aliquots of sCS solution (10 mg/mL in 0.3 M Na_2SO_4 mobile phase) were applied into the GPC-HPLC system at a flow rate of 1 mL/min. UV detection was performed at 205 nm at room temperature. The column was previously calibrated with polysaccharides of known molecular weights; 1.7, 4.0, 10.0 and 16.0 kDa,

corresponding to fondaparinux sodium, enoxaparin, heparan sulfate and unfractionated heparin, respectively.

5. Structural characterization

Enzymatic digestion was performed as previously described by Lima et. al., 2013. Briefly, 100 μg of the isolated compound were incubated overnight with chondroitinases ACII and ABC together (2.5 mIU each − TRIS-HCl PH 8.0, 60 mM sodium acetate). The disaccharides produced by exhaustive action of chondroitin ACII and ABC lyases on the chondroitin sulfate from *L. vannamei* and a mixture of disaccharide standards were resolved on a high performance liquid chromatography (HPLC) with 150×4.6 mm Phenosphere SAX column (Phenomenex, Torrance, CA, USA). The column was eluted with a NaCl gradient of 0–1 M during 30 min with a 1 mL/min flux and UV detection at 232 nm. The peaks corresponded to the elution positions of known disaccharide standards as follows: ΔUA β (1→3) GalNAc 6-O-sulfate; ΔUA β (1→3) GalNAc 4-*O*-sulfate; ΔUA β(1→3) GalNAc 4,6-di-*O*-sulfate. However, resistance to chondroitinase digestion has been reported (Sugahara et. al., 1996) and further investigations employing NMR spectroscopy were also undertaken.

NMR experiments were performed on sCS in 200 μL of D_2O containing 100 μM DSS at 343 K using a 600 MHz Bruker Avance II+ spectrometer fitted with a TCI CryoProbe. In addition to 1-dimensional (^{1}H and ^{13}C) spectra, both homonuclear (COSY, TOCSY and NOESY) and heteronuclear (HSQC and HMBC) 2-dimensional spectra were collected. TOCSY spectra were measured with a 120 ms mixing time while the mixing times for NOESY spectra were between 30 and 240 ms. Spectra were processed using Bruker TopSpin and assigned using the Collaborative Computing Project for NMR Analysis software (Vranken et al., 2005). ^{1}H/^{13}C HSQC integration was performed using the INFOS spectrum fitting software (Smith, 2017). Proton spectrum integration was performed using Bruker TopSpin software to calculate the proportion of each residue variant present within the polysaccharide sample. Full acquisition parameters are provided in Supplementary Data, Table ST1.

6. Anticoagulant Activity assays

Activated partial thromboplastin time (aPTT) assays were carried out according to the aPTTest manufacturer's instructions (Labtest, Lagoa Santa, MG, Brazil). Unfractionated Heparin and sCS were diluted in saline and incubated with 90 μL of plasma and 100 μL of cephalin at 37 °C for 3 minutes. CaCl$_2$ was added and the coagulation time was measured. The anti-IIa and anti-Xa activities were performed in 96-well microplate according to the kit instructions Actichrome heparin (anti-fIIa) (American diagnostica Inc. Greenwich, CT, USA) and Biophen heparin anti-Xa kit (HYPHEN Biomed, ref: 221010), respectively. Antithrombin and thrombin were incubated with mammalian heparin or purified sCS at various concentrations at 37 °C for 2 min. After incubation, purified bovine factors Xa or IIa were added, mixed and incubated at 37 °C for 2 min. Next, the chromogenic substrate for factors Xa or IIa were added and the mixture incubated again for 2 min at 37 °C. Then, to stop the reaction, 30% acetic acid was added and absorbance measured at 405 nm against a corresponding blank using a microplate reader (BioTek Epoch, Winooski, USA). A thrombin inhibition HCII-mediated assay was performed with the following reagents: 70 nM heparin cofactor II, 15 nM thrombin and 0-100 μl of the test sample and heparin in 25 μl of 0.02 M Tris/HCl, 0.15 M NaCl (pH 7.4). Then, 25 μL of thrombin were added and incubated for 1 minute at 37 ºC. Thereafter, 25 uL of the chromogenic substrate N-benzoyl-Phe-Val-Arg-*p*-nitroamilidahydrochloride (100 mM) were added and the mixture was incubated for 1 minute at 37 °C. 25 μL of 30% acetic acid were added to stop the reaction and the absorbance was read at 405 nm.

7. Bleeding effect

The residual hemorrhagic effect of the sample was analyzed by a modified model of topical scarification in rat tail (Cruz & Dietrich, 1967). A scarification was made (surgical blade) in the distal portion of the rat tail. Next, the scarified tail was dipped vertically in physiological saline solution, and dipped again in fresh saline to observe bleeding. Then, the tail was dipped in a solution containing the sCS or heparin at different concentrations over 2 mins and washed extensively with saline solution. The treated tail was immersed in new saline solutions over 40 mins, and the amount of protein from the lesion was determined by Bradford assay (Bradford, 1976). The results

were expressed as the sum of the protein values of each tube minus the amount of protein present before the exposure to the test substance.

8. LPS-induced peritonitis

C57BL/6 mice were injected with 100 μL of lipopolysaccharide (LPS, 055:B5 strain, 3.3 mg Kg^{-1}) or Phosphate-buffered saline (PBS), referred as 'PBS control group', into the peritoneal cavity. After 15 minutes, animals induced with LPS were injected intravenously with mammalian heparin, sCS (300 μg Kg^{-1} in PBS) or PBS alone (treatment control), referred as 'PBS group'. 4 hours later, the peritoneal cavity was washed with 2 mL of PBS containing 0.5 % bovine serum albumin and 1 mM ethylenediaminetetraacetic acid (EDTA) in PBS. The total number of cells in the peritoneal lavage fluid was measured by hemocytometer. The differential count of polymorphonuclear leukocytes (PMN) was determined by cytospin preparations fixed with hematoxylin and eosin.

9. Cytokine quantification

The peritoneal liquid of each treated group was collected after 4 hours of induction of inflammation with LPS and stored at -80 °C. The IL-1β, IL-6 and TNF-α levels were measured using enzyme immunoassay kit (ELISA) (eBioscience, San Diego, CA, USA) according to the manufacturer's instructions. Each sample was measured in triplicate and the optical density of each well (assay performed in 96 well plates) was determined at 450 nm.

10. Cell viability assay

RAW 264.7 cell viability was determined by the MTT (3- (4,5-Dimethylthiazol-2-yl) -2,5-bromo diphenyltetrazolium) method (Mosmann, 1983). Cells were plated in 24 well plates (4.8 x 10^5 cells per well) and treated with different concentrations of GAGs. After 24 hours 350 μL per well of MTT solution (5 mg/mL)

were added. After 4 hour of incubation, cell supernatant was removed and 500 µL of dimethylsufoxide (DMSO) were added to all wells to lyse the cells and solubilize the crystals. The absorbance was determined at 570 nm.

11. Nitric Oxide production quantification

RAW 264.7 cells (4.8×10^5 cells.$100\mu L^{-1}$) were plated and induced with LPS (O55:B5 strain) and 1 hour later, treated with sCS or heparin (0.1, 1.0, 10 and 100 µg/mL). After 24 hours, the supernatant was aspirated and submitted to nitric oxide (NO) dosage. In order to determine the total NO concentration, 50 µL of Griess reagent (1% sulfanilamide in 5% phosphoric acid and 0.1% naphthylethylenediamine dihydrochloride in water) were added to 50 µL of cell supernatant from each well. After 30 minutes of incubation at room temperature, the absorbance was determined at 545 nm with a microplate reader.

12. Statistical analysis

Results were analyzed by two-way ANOVA and Bonferroni post-test and post-hoc Tukey test. Values of $p < 0.01$ and < 0.001 were considered indicative of statistical significance.

Results and discussion

1. Structural characterization

The sCS from the shrimp cephalothorax isolated and fractionated as described above was purified using ion-exchange column, eluting with a NaCl stepwise (0.5 M; 0.8 M and 1.0 M) gradient. The sub-fraction eluting at 1.0 M NaCl, provided the sCS sample of the present study, which was then subjected to structural characterization. The molecular weight (M_w) was determined by GPC-HPLC as 12 kDa, corresponding to just under half of the average molecular weight (26 kDa) for another sCS isolated from *L. vannamei* shrimp under distinct conditions (Cavalcante et. al., 2018) and for bovine tracheal CS (Tomatsu, 2015). The present polysaccharide also differs from other CS

polysaccharides in terms of its composition and chain length (Sugahara et. al., 2003). Following treatment with chondroitinases ACII and ABC, products comprised 25.9 % of ΔU-GalNAc non-sulfated and 74.1 % of disaccharides bearing a sulfate ester at 4 or 6 positions and both 4,6 (ΔU-GalNAc-4-*O*-sulfate; ΔU-GalNAc-6-*O*-sulfate and ΔU-GalNAc-4,6 di-*O*-sulfate, respectively) (Fig.S2).

Although the presence of significant proportions of the disaccharide ΔU-GalNAc-4,6 di-*O*-sulfate by chondroitinase digestion and HPLC initially suggested a so-called CS-E type structure, following NMR, other structures were evident and these were investigated further.

Structural characterization was performed using a combination of 1-dimensional (^{1}H and ^{13}C), homonuclear 2-dimensional (COSY, TOCSY and NOESY) and heteronuclear 2-dimensional (HSQC and HMBC) NMR spectroscopy. The assignments for the hydrogen and carbon resonances and the chemical shift map of ^{1}H/^{13}C atoms (2-dimensional ^{1}H/^{13}C HSQC) are shown in Fig. 1. NMR characterization generated ^{1}H and ^{13}C assignments for eight constituent monosaccharide variants termed here; GlcA, GlcA-3S*i*, GlcA-3S*ii*, GalNAc4S*i*, GalNAc-4S*ii*, GalNAc-6S*i*, Gal-NAc-6S*ii* and GalNAc-4,6S present in the 2-dimensional ^{1}H/^{13}C HSQC spectrum (Fig. 1), where 'S' represents–*O*-sulfate and the superscripts *i* and *ii* denote signals from the same residue type, but in slightly different environments (most likely distinct adjacent residues). GlcA β(1→3) GalNAc linkages evident in both ^{1}H/^{1}H NOESY and ^{1}H/^{13}C HMBC spectra reveal four disulfated and one trisulfated disaccharide variants (continuing the nomenclature used above); GlcA β(1→3) GalNAc-4,6S, GlcA-3S*i* β(1→3) GalNAc-4S*i*, GlcA-3S*i* β(1→3) GalNAc-4S*ii*, GlcA-3S*i* β(1→3) GalNAc-4,6S and GlcA-3S*ii* β(1→3) GalNAc-6S*i*. Inter-disaccharide linkages, GalNAc β(1→4) GlcA, were also observable in the ^{1}H/^{1}H NOESY and ^{1}H/^{13}C HMBC spectra between GalNAc-4S*i* and GlcA, GalNAc-4S*ii* and GlcA-3S*i*, GalNAc-4,6S and GlcA-3S*ii*, GalNAc-6S*i* and GlcA and GalNAc-6S*ii* and GlcA. The unusual GlcA-3S residue was identified through characteristic chemical shifts patterns in agreement with the literature (Ustyuzhanina et al., 2016). The proportions for each of the five constituent residues identified were determined from the ^{1}H/^{13}C HSQC spectrum. Integration of the key anomeric signals (between 4.4-4.7 ppm in ^{1}H and 102-108 ppm in the ^{13}C dimension) indicated a composition of: GlcA 40.4%, GlcA-3S 59.6% and GalNAc-4S 46.2%, GalNAc-6S 2.5% and GalNAc-4,6-diS 28.3%.

The GlcA β(1→3) GalNAc-4,6S disaccharide linkage was ascertained from cross peaks present at 4.472, 4.012 ppm of NOESY spectra collected with NOE interaction times of 120 and 240 μs. This linkage was further identified via cross peaks present in the HMBC spectrum at 4.472, 79.10 and 4.016, 106.68 ppm. Similarly, linkages present within the GlcA-3S*i* β(1→3) GalNAc-4S*i*, GlcA-3S*i* β(1→3) GalNAc-4S*ii* and GlcA-3S*i* β(1→3) GalNAc-4,6S disaccharides were also observed via NOESY cross peaks at 4.593, 3.997; 4.593, 3.986 and 4.593, 4.010 ppm respectively, however, these were partially overlapping. Two broad HMBC cross peaks, covering the region of the GlcA-3S*i* linkage with GalNAc-4S*i*, -4S*ii* and -4,6S, were present at 4.593, 79.11-80.01 and 3.968-4.018, 106.64 ppm suggesting a linkage between these residues, but they were not resolved into three pairs of cross peaks. The combination of NOESY and HMBC spectra also indicated GlcA-3S*ii* β (1→3) GalNAc-6S*i* disaccharide linkages via NOESY cross peaks at 4.550, 3.801 and 4.555, 3.698 ppm respectively. The NOESY cross peak for the GlcA-3S*ii* β (1→3) GalNAc-6S*i* disaccharide linkage was supplemented by HMBC cross peaks at 3.802,106.54 and 4.546,83.72 ppm.

No signals corresponding to the disaccharides containing GlcA-2,3S were identified. This residue has been reported as part of another naturally-occurring CS from the same organism that was isolated under different conditions (Cavalcante et. al., 2018) and as the chemically over-sulfated CS, which was a contaminant of pharmaceutical heparin (Guerrini et al., 2008), but the characteristic ^{1}H and ^{13}C signals are not present in the present sample, thereby establishing the unique character of the present sCS polysaccharide.

Chondroitin sulfate chains containing 3-*O*-sulfated GlcA are resistant to the action of chondroitinase AC-II, and chondroitinase ABC digestion of such oligosaccharides has been reported to result in the apparent disappearance of 3-*O*-sulfated GlcA containing disaccharide residues (Sugahara et. al., 1996). Thus, it is likely that after chondroitinase ACII and ABC treatment of the present sCS polysaccharide that significant portions of the molecule remain undigested and are not be detected by absorbance at 232 nm on HPLC. In contrast, NMR analysis permitted all structural variants to be detected and, through correlation spectra, their assignments to be made (Table 1), even for previously rarely-reported substituents, such as the 3-*O*-sulfated

glucuronic acid the chemical shift patterns allowing sulfated positions to be inferred owing to the highly electronegative properties of the sulfate group.

The natural occurrence of 3-*O* sulfated GlcA residues in CS chains is rare and it has been reported in only a few marine animal sources (Kitagawa, 1997; Mou et. al., 2018; Sugahara at. al., 1996; Shetty et. al., 2009; Ustyuzhanina et al., 2016), suggesting that this pattern may require a specific enzyme. It has been shown that 3-*O*-sulfate groups at the non-reducing terminal GlcA residue of trombomodulin from human urine samples can be recognized by an HNK-1 (human natural killer-1) monoclonal antibody (Nadanaka et. al., 1998). Recently, HNK-1 sulfotransferase (HNK-1ST) that catalyzes 3-*O*-sulfation of terminal GlcA in the HNK-1 carbohydrate antigen precursor has been also shown to be involved in the 3-*O*-sulfation of the linkage region of GlcA, leading to the generation of an unique HNK-1 epitope (Hashiguchi et. al., 2011; Nakagawa et. al., 2011). 3-*O*-sulfated GlcA residues were described in other glycoproteins and glycolipid saccharide sequence in mammals (Ilyas, Dalakas, Brady, & Quarles, 1986). In all cases, it has been shown that this unique sulfation pattern requires the same 3-*O*-sulfotransferase (Hashiguchi et. al., 2011; Nakagawa et. al., 2011), however, so far, no 3-*O*-sulfotransferase responsible for the 3-*O*-Sulfation pattern in GlcA residues has been characterized for CS molecules obtained from marine sources. The CS biosynthesis is dictated by multiple enzymes, which can display organism-type specific patterns of expression, potentially leading to functional diversity of CSPGs among different animal species. The peculiar structural features of these compounds distinguish the biosynthetic process from the classical model of GAG biosynthesis, suggesting a relation between the pattern of GAG sulfation and animal evolution.

Fig. 1. A ^{1}H/^{13}C HSQC spectrum of sCS with 1-dimensional ^{1}H and ^{13}C external projections obtained at 600 MHz in D$_{2}$O at 343 K and referenced to 100 μM DSS. The letter G represents glucuronic acid and 3-*O*-sulfate groups are indicated by superscript 3S while the letter A (aminosugar) represents N-acetyl β-D-galactosamine with 4-*O*-, 6-*O*- and 4,6 di-*O*-sulfate groups indicated by superscripts 4S, 6S and 4,6S respectively. The superscripts *i* and *ii* represent the same residue type with different neighbouring residues, hence slightly different chemical shifts. Minor signals, including unsulfated GalNAc can also be detected (Supplementary Data Information).

Table 1. ^{1}H and ^{13}C NMR HSQC assignments of sCS from *Litopenaeus vannamei* (Values in ppm at 70 °C).

Residue		1	2	3	4	5	6		-COCH$_3$
GlcA	^{1}H	4.467	3.388	3.570	3.788	3.704	---	---	---
	^{13}C	106.681	75.367	76.846	83.749	79.557	---	---	---
GlcA-3S*i*	^{1}H	4.589	3.647	4.376	4.048	3.773	---	---	---
	^{13}C	106.637	75.301	84.947	80.998	80.025	---	---	---
GlcA-3S*ii*	^{1}H	4.551	3.625	4.372	4.052	3.829	---	---	---
	^{13}C	106.506	75.301	84.269	79.993	79.988	---	---	---
GalNAc-4S*i*	^{1}H	4.596	3.991	3.996	4.727	3.803	3.834	3.759	2.020
	^{13}C	104.028	54.773	79.347	79.429	77.665	64.173	64.151	25.702
GalNAc-4S*ii*	^{1}H	4.633	4.034	3.986	4.757	3.736	3.785	3.730	2.020
	^{13}C	104.295	54.695	79.724	79.361	77.595	64.147	64.100	25.702
GalNAc-6S*i*	^{1}H	4.547	3.987	3.804	4.126	4.031	4.207	4.167	2.020

	¹³C	104.109	54.018	83.825	70.572	78.692	70.391	70.400	25.702
GalNAc-6S*ii*	¹H	4.577	3.996	3.692	4.136	4.076	4.269	4.208	2.020
	¹³C	104.503	54.001	77.909	70.232	75.566	70.905	70.837	25.702
GalNAc-4,6S	¹H	4.671	4.007	4.006	4.778	3.962	4.268	4.241	2.020
	¹³C	103.223	54.734	79.114	79.480	75.405	70.120	70.078	25.702

[1]Combined values for signals denoted *i* and *ii* in HSQC spectrum (Figure 1).

2. Effect on coagulation time and mediators

The anticoagulant activity of GAGs seems to be related, besides the degree of sulfation, to differences of GAG-ligand proteases or conformational changes during GAG-protein interactions (Nandini & Sugahara, 2006; Tiedemann et. al., 2005). The clotting time of sCS was investigated using an aPTT test, which assesses the intrinsic pathway of the coagulation cascade and by factor IIa and Xa directly and HCII-mediated inhibition chromogenic assays. In the aPTT assay, sCS presented reduced anticoagulant activity (30 UI.mg⁻¹) compared to commercial heparin (190 UI.mg⁻¹), known for its high anticoagulant activity (Brito et. al., 2014) (Fig.2). A CS from the smooth hound shark (*mustelus*) composed mainly of monosulfated disaccharides in position 6 and 4 of the *N*-acetyl β-D-galactosamine (Krichen et. al., 2018), showed six times lower anticoagulant activity compared to sCS.

Unlike heparin and its mimetics, which are capable of binding to both HCII and antithrombin and inhibiting proteases, the anticoagulant activity of CS usually arises through direct and HCII-mediated inhibition of thrombin (Casu, Guerrini, & Torri, 2004; Karamanou et. al., 2017. In order to investigate the ability of sCS to promote FII inhibition chromogenic assays were carried out and the sCS achieved 80% anti-IIa activity at 1.0 μg/mL (Fig.3A). A similar effect (96% inhibition) was observed for a previously reported sCS (Cavalcante et. al., 2018), suggesting a particular anti-thrombin activity for marine CS that could be related, not only to coagulation mechanisms, but also to other biological effects displayed by marine CS. Furthermore, although Xu and co-workers (Xu et. al., 2018) describe that the degree of fucosylation is an important feature for the anti-HCII-mediated thrombin activity of CS compounds, the sCS has achieved about 90% of anti-HCII-mediated thrombin activity at 100 μg/mL concentration (Fig.3B). Another protease that plays an important role in anticoagulant

activity, factor Xa, was evaluated. Figure 3C shows that the anti-Xa activity of sCS is notably lower than heparin, probably due to its inability to interact and stabilize AT (Fig.4). It was previously reported that there is a close relationship between AT thermal stabilization and anticoagulant activity of polysaccharides (Lima et al., 2013). These data could explain the moderate anticoagulant activity seen in the aPTT test. Similarly, no anti-Xa effect was described for other forms of sCS from *L. vannamei* (Cavalcante et al., 2018), suggesting a particular anticoagulant route for marine CS. Together, these findings emphasize the complex multifactorial relationships implicated in the inhibitory activities of sCS on the different mechanisms of blood coagulation.
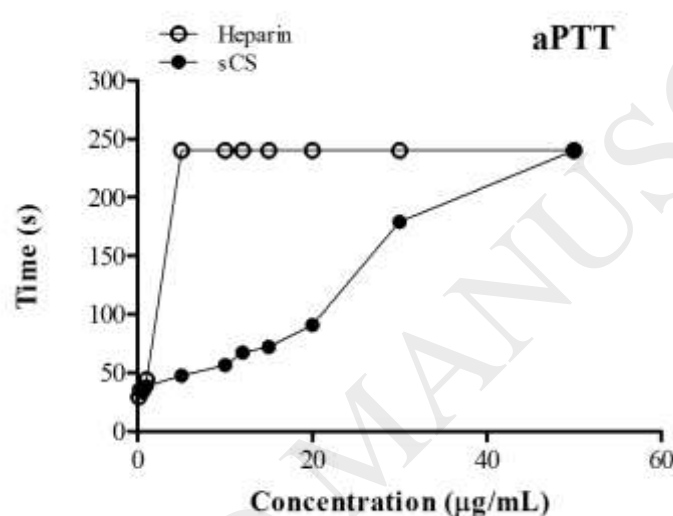
Fig. 2. Anticoagulant activity of sCS (●) and unfractionated heparin (○) measured by activated partial thromboplastin time (aPTT). Values are the mean of three independent experiments.
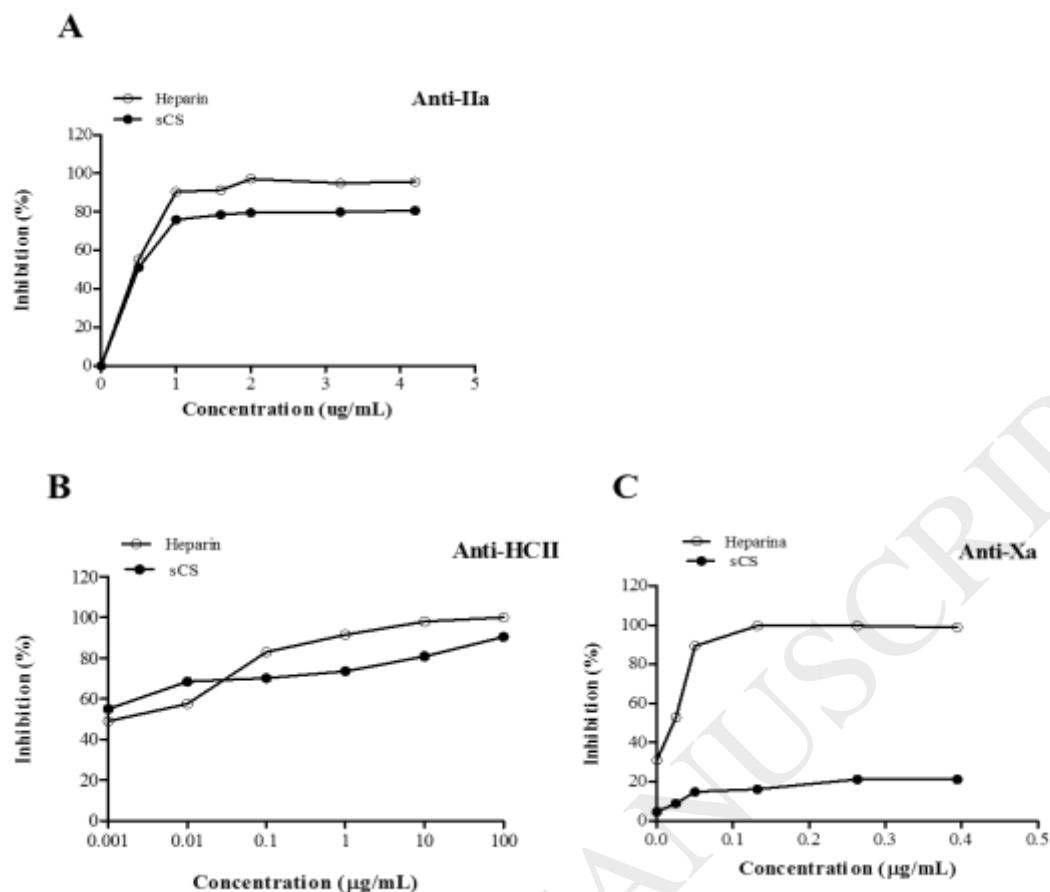
Fig. 3. Anti-IIa activity (A), thrombin inhibition mediated by HCII (B) and anti-Xa activity (C) of sCS (●) and unfractionated heparin (○).The tests were conducted using chromogenic methods as mentioned in methods. Values are the mean of three independent experiments.
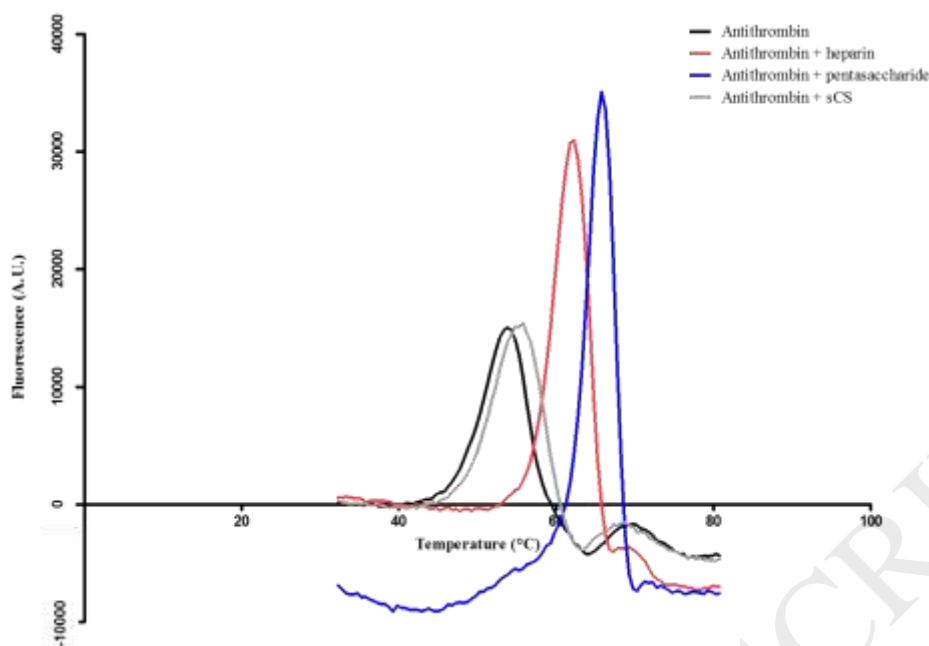
Fig. 4 Effect of sCS on thermo-stabilization of antithrombin evaluated by differential scanning fluorimetry. Melting curve profile (first derivative) of 30 nM antithrombin in the presence or absence of different ligands. Antithrombin (black solid line); antithrombin+sCS (grey solid line); antithrombin+heparin (red solid line); antithrombin+pentasaccharide (blue dotted line).

3. Hemorrhagic effect

Since the use of unfractionated heparin leads to disturbances in hemostasis, leading to hemorrhagic events, the residual hemorrhagic effect of sCS was investigated. Even at 5 times higher concentration (500 μg/mL), sCS exhibited no significant change in its effect on the residual bleeding when compared to its effect at lower concentration (100 μg/mL), showing almost no hemorrhagic activity (Fig.5). The strong binding of heparin to myosin ATPase receptors that were exposed during wounding, results in uncontrollable bleeding. The insignificant hemorrhagic activity presented by this sCS could be explained by the lack of binding or interaction to these receptors. Such a feature of sCS suggests that this compound has minimal bleeding effects. The structural differences of these GAGs influence their abilities to bind and control the functional interactions with biologically important proteins (Pomin & Mourão, 2014). Although various GAG structures have been characterized in several marine animals, including other *L. vannamei* GAGs (Brito et al., 2008, 2014; Cavalcante et. al. 2018; Chavante et

al., 2014), the biological roles of these unique structures have not been yet fully disclosed.
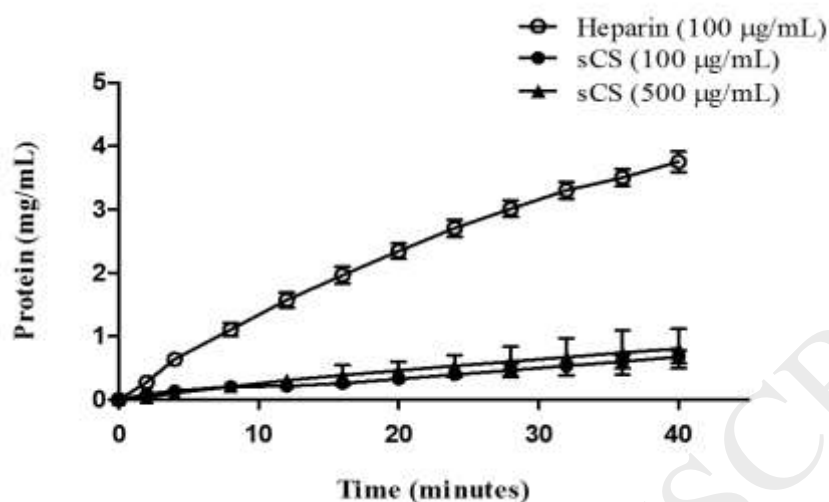
Fig. 5. Hemorrhagic activity in a rat-tail scarification model. 100 μg/mL (●) and 500 μg/mL of sCS (▲) or unfractionated heparin (○) was applied topically and the bleeding potency measured after 2 min following up to 40 min. The bars indicate the standard error of the measurements.

4.   Effect on LPS-induced peritonitis and cytokine production

The structural peculiarity of CS enables it to display a wide range of biological activities, including anti-inflammatory effect (Lauder, 2009; Volpi, 2011). Previously, CS compounds obtained from several marine sources have been studied as potential anti-inflammatory agents (Cunha et. al., 2017; Krylov et. al., 2011; Mou et. al., 2018; Ustyuzhanina et. al., 2018).

In this context, the *in vivo* anti-inflammatory effect of sCS was evaluated. The analysis of total leukocytes present in the peritoneal lavage showed a three-fold decrease in mice treated with sCS or heparin compared to untreated animals (PBS and PBS control groups)   (Fig. 6A). The sCS showed significantly reduced leukocyte recruitment, mainly PMN in approximately 60%, compared to the PBS group, while heparin achieved only 30% inhibition (Fig. 6B). Another GAG obtained from the same shrimp, also inhibited the leucocyte infiltration, as well as the activity of enzymes involved in this process (metalloproteinase 9 and pro-metalloproteinase 2) (Brito et. al., 2008). Moreover, 45% of migratory inhibition were observed for a fucosylated CS

obtained from *Cucumaria djakonovi* sea cucumber, while a low fucosyl branched CS from another sea cucumber species presented 31% of leukocyte recruitment inhibition (Ustyuzhanina et. al, 2018). The interesting fact is that sea cucumber CS shares the presence of GalNAc-4,6 di-*O*-sulfate with this form of sCS. However, although the presence of fucosyl branches and a higher degree of sulfation are often reported as essential structural features for the more pronounced anti-inflammatory effects of CS compounds, the high PMN inhibition activity of this sCS suggests that there are other biochemical characteristics involved in this effect.

There is supporting evidence that signaling through coagulation proteases makes an important contribution to the inflammatory response (Foley & Conway, 2016). As the main coagulation protease, thrombin is capable of inducing the expression of a variety of biological molecules mediated by PAR receptors modulating physiological and pathological process such as inflammation and cancer development, respectively (Coughlin, 2000; Zigler et. al. 2011). During the inflammation process, thrombin activates PAR-1, its signaling triggers the expression of pro-inflammatory cytokines (such as IL-1β, IL-6 and IL8), chemokines (such as MCP-1) and cell adhesion molecules, promoting the activation of leukocytes, leading to attachment, rolling and adhesion to endothelial surface, thus contributing to leukocyte recruitment (Foley & Conway, 2016; López et. al., 2014; Strande & Phillips, 2009).

Furthermore, it is known that GAGs, including CS compounds are capable of binding cytokines, thereby mediating inflammatory responses (Lever, Mulloy, & Page, 2012). Therefore, pro-inflammatory cytokine levels were quantified from peritoneal liquid. In animals treated with sCS, cytokine levels were sigficantly reduced, almost reaching the basal cytokines levels found for the PBS control group (healthy animals). IL-1β levels were about 64 % lower compared to PBS-treated animals, while for TNF-α, the inhibition was approximately 82 % (Fig. 7). Inhibitory activity was also observed for IL-6 levels, in which the sCS reached about 64 % inhibition compared to the PBS group. The LPS injected into animals is adsorbed through interstitial fluid and serum and is degraded into the *O*-antigen, core protein and lipid-A, which is highly pro-inflammatory. Lipid-A binds the CD14/TLR4/MD2 receptor of tissue macrophages and serum monocytes to trigger the activation of NF-κβ protein family, via a complex multiple step intracellular process, initiating the production of pro-inflammatory

cytokines, such as TNF-α, IL-1β, IL-6 and IL8 (Jaffer, Wade & Gourlay, 2010; Lawrence, 2009).

The binding of cytokines to different GAGs is well-known and a minimal chain length seems to be required for this interaction. Mammalian CS has an IC_{50} value of 22 mg/mL in cytokine interactions (Kuschert et. al., 1999). In joints, CS can reduce the concentrations of pro-inflammatory cytokines, such as TNF-α (Campo et. al., 2003) and IL-1β (Chou et. al., 2005). The link between coagulation and inflammatory process seems to have a refined molecular basis. Thrombin-treated monocytes exhibited increased transcriptional activation of NF-Kβ p50/p65, a triggering factor of inflammatory process (Zhang, 2010). These data could suggest a mechanism which by those compounds modulate their anti-inflammatory effect, either by direct cytokine-binding or thrombin inhibitory signaling, such as activation of transcriptional factors involved in regulation of the immune response.
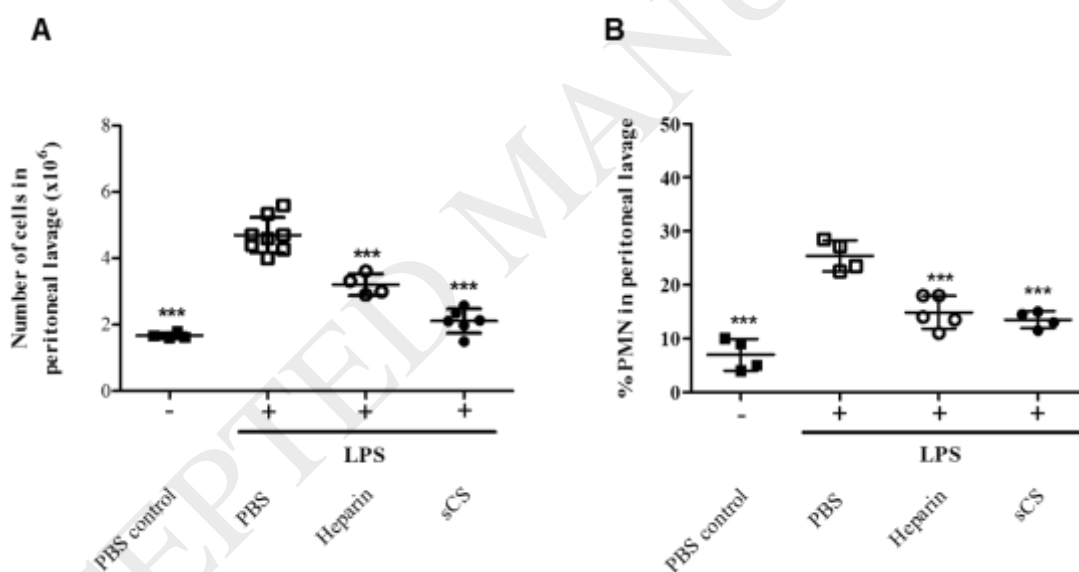
Fig. 6. Polymorphonuclear cells (PMN) recruitment, in an inflammation model of peritonitis LPS-induced is inhibited by sCS. The mice were treated intraperitoneally with 100 μl of LPS 15 min before the intravenous injection of sCS, unfractionated heparin (300 µg Kg^{-1}), or no treatment (PBS control group). After 4 hours, the peritoneal lavage fluid was evaluated for total cell number (A) and the percentage of PMNs (B). PMNs were identified by staining with hematoxylin and eosin. Statistical significance was determined by ANOVA (two-way) test and Bonferroni post-test (***p <0.001). The bars indicate the standard error of the measurements. Bar: 20 µM.
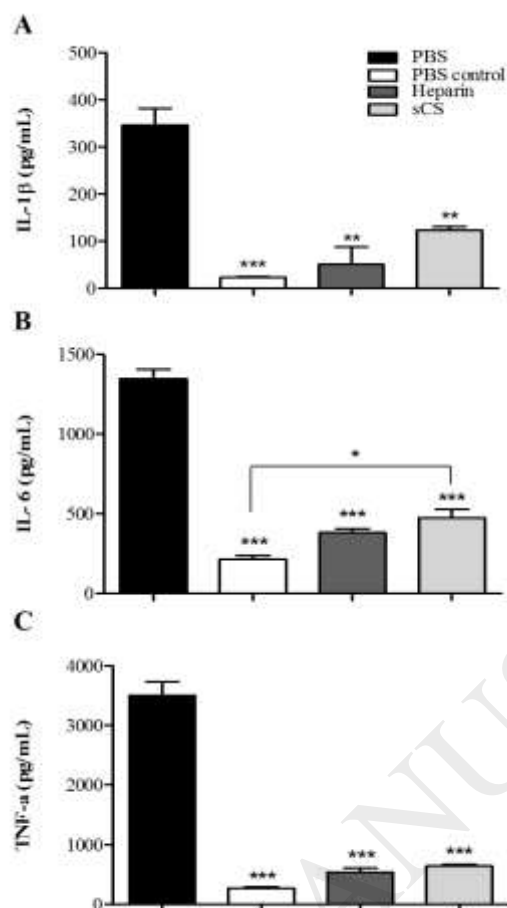
Fig. 7. IL-1β (A), IL-6 (B) and TNF-α (C) levels production stimulated by LPS in C57BL/6 mice after treatment with shrimp sCS, unfractionated heparin or no treatment (PBS). The results represent the average levels of cytokine (pg/ml) and standard deviations of the animals in each group when compared with each cytokine control. Statistical significance was determined by ANOVA (one-way) test and post-hoc Tukey test (** $p < 0.01$; *** $p < 0.001$). The bars indicate the standard error of the measurements.

5. Inhibition of *in vitro* NO production and RAW 264.7 cell viability

The rise in NO levels is stimulated through TNF-α production, activating a variety of biological effects such as platelet activation, bactericidal potential and immune system modulation (Bogdan, 2015). Once TNF-α production is inhibited, a decrease in NO levels was also expected. Thus, the NO production by macrophages was measured in the presence of different concentrations of the compounds. Both heparin and sCS reduced the NO production by macrophages at all tested dosages, however, at 100 μg/mL, sCS achieved 55 % and heparin, 43 %, inhibition (Fig.8A). Importantly, this inhibition was not induced by cell toxicity, since the MTT viability test demonstrated that none of the GAG concentrations evaluated were able to induce cell death (Fig. 8B).

Although it is clear that the GAGs bind to cytokines, it is still unclear which structural properties provide the high NO inhibiton potential of this polysacharide. Differences in chain length, disaccharide compositon or sulfation pattern might be implicated in these distinct biological activities. A fucosylated CS isolated from sea cucumber has exhibited similar NO reduction in a hepatic endoplasmatic reticulum stress-associated inflammation assay in obese mice (Hu et. al., 2015). These findings indicate that there are some notable characteristics among GAGs from marine sources, that remain to be unveiled.
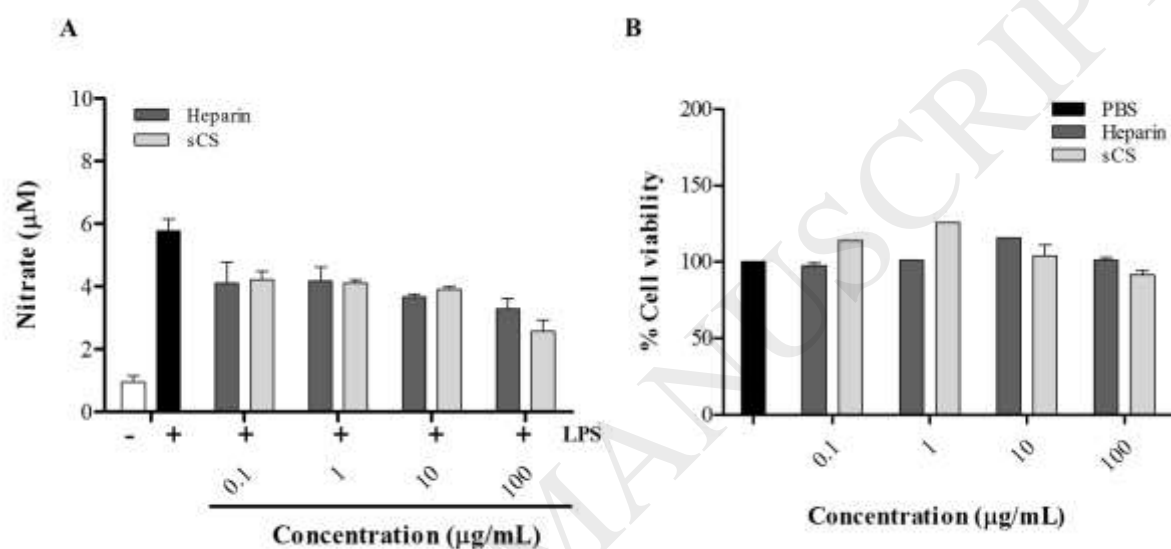
Fig. 8. Effects of unfractionated heparin and sCS on nitrite (NO) production in LPS-stimulated RAW 264.7 macrophages. NO production was measured by the Griess reaction assay and expressed as a percentage of control (LPS alone) (A). Effects of GAGs on cell viability. Cell viability was evaluated by MTT assay 24 h after GAG treatment in RAW264.7 macrophages (B). Values are the mean $\pm$ SD of the three independent experiments. Statistical significance was determined by ANOVA (two-way) test and Bonferroni post-test (* $p < 0.05$; ** $p < 0.01$). The bars indicate the standard error of the measurements

Conclusion

Studies on the anti-inflammatory effects of non-fucosylated CS compounds are still scarce. The biological properties herein presented by the present sCS suggest its importance within the context of inflammation and hemostasis. Although oversulfated CS products derived from semi-synthetic routes were associated with the heparin

contamination crisis (Guerrini et. al., 2008), the peculiar structural composition of sCS (lacking 2, 3 di-sulfated GlcA residues or extensive per-sulfation of GalNAc residues) and the interesting biological effects reported here for this form of sCS suggest it as a biotechnological target for further exploration of the relationships between structure and function of GAGs.

Addendum

Each author contributed to the development of the manuscript and reviewed of each draft, and approved the final draft. L. C. G. F. Palhares conducted the *in vivo* and *in vitro* studies. A. S. Brito and S. F. Chavante contributed to the study design. J. London, I. Barsukov, M. A. Lima and H. B. Nader contributed to acquisition and analysis of structural data. E. A. Yates, G. P. V. Andrade and S. F. Chavante contributed to data interpretation.

Acknowledgements

Disclosure of Conflict of Interests

The authors state that they have no conflict of interest.

References

Bradford, M. M. (1976). A rapid and sensitive method for the quantitation of microgram quantities of protein utilizing the principle of protein-dye binding. *Analytical Biochemistry*, **72**, 248–254.

Brito, A. S., Arimateia, D. S., Souza, L. R., Lima, M. A., Santos, V. O., Medeiros, V. P., et al. (2008). Anti-inflammatory properties of a heparin-like glycosaminoglycan with reduced anti-coagulant activity isolated from a marine shrimp. *Bioorganic & Medicinal Chemistry*, **16(21)**, 9588–9595.

Brito, A. S., Cavalcante, R. S., Palhares, L. C., Hughes, A. J., Andrade, G. P., Yates, E. A., et al. (2014). A non-hemorrhagic hybrid heparin/heparan sulfate with anticoagulant potential. *Carbohydrate Polymers*, **99**, 372–378.

Bogdan, C. (2015). Nitric oxide synthase in innate and adaptive immunity: an update. *Trends in Immunology,* **36**: 161-178.

Campo G. M, Avenoso A, Campo S, Ferlazzo A. M, Altavilla D, Calatroni A. (2003). Efficacy of treatment with glycosaminoglycans on experimental collagen-induced arthritis in rats. *Arthritis Research*, **5,** 122-131.

Casu, B., Guerrini, M. & Torri, G. (2004). Structural and Conformational Aspects of the Anticoagulant and Antithrombotic Activity of Heparin and Dermatan Sulfate. *Current Pharmaceutical Design*, **10(9)**, 939-949.

Cavalcante, R. S, Brito, A. S., Palhares, L. C., Andrade, M. L., Cavalheiro, R. P., Nader, H. B., Sassaki, G. L., Chavante, S. F. (2018). 2,3-Di-*O*-sulfo glucuronic acid: An unmodified and unusual residue in a highly sulfated chondroitin sulfate from *Litopenaeus vannamei Carbohydrate Polymers*, **183**, 192–200.

Chavante, S. F., Brito, A. S., Lima, M., Yates, E., Nader, H., Guerrini, M., et al. (2014). A heparin-like glycosaminoglycan from shrimp containing high levels of 3-O-sulfated D-glucosamine groups in an unusual trisaccharide sequence. *Carbohydrate Research*, **390**, 59–66.

Chou M. M, Vergnolle N, McDougall J. J, Wallace J. L, Marty S, Teskey V., et al. (2005). Effects of chondroitin and glucosamine sulfate in a dietary bar formulation on inflammation, interleukin-1beta, matrix metalloprotease-9, and cartilage damage in arthritis. *Experimental Biology and Medicine*, **230**, 255-62.

Coughlin, S. R. (2000). Thrombin signalling and protease-activated receptors. *Nature*, **407**: 258–264.

Cruz, W. O., & Dietrich, C. P. (1967). Antihemostatic effect of heparin counteracted by adenosine triphosphate. Proceedings of the Society for *Experimental Biology and Medicine*, **126(2)**, 420–426.

Cunha, A. L., Aguiar, J. A. K., Silva, F. S. C., Michelacci, Y. M. (2017). Do chondroitin sulfates with different structures have different activities on chondrocytes and macrophages? *International Journal of Biological Macromolecules*, **103**, 1019–1031.

Dietrich, C. P., & Dietrich, S. M. C. (1976). Electrophoretic behaviour of acidic mucopolysaccharides in diamine buffers. Analytical Biochemistry, 70(2), 645–647.

Deepa, S. S., Yamada, S., Fukui, S. and Sugahara, K. (2007). Structural determination of novel sulfated octasaccharides isolated from chondroitin sulfate of shark cartilage and their application for characterizing monoclonal antibody epitopes. *Glycobiology*, **17(6)**, 631-45.

Foley, J. H. & Conway, E. M. (2016). Cross Talk Pathways Between Coagulation and Inflammation. *Circulation Research*, **118**:1392-1408.

Guerrini, M., Beccati, D., Shriver, Z., Naggi, A. M., Bisio, A., Capila, I., et al., (2008) Oversulfated chrondroitin sulfate is a contaminant in heparin associated with adverse clinical events. *Nature Biotechnology*, **26**, 669-675.

Hashiguchi T., Mizumoto S., Nishimura Y., Tamura J., Yamada S., Sugahara K. (2011) Involvement of human natural killer-1 (HNK-1) sulfotransferase in the biosynthesis of the GlcUA(3-O-sulfate)-Gal-Gal-Xyl tetrasaccharide found in α-

thrombomodulin from human urine. *Journal of Biological Chemistry*, **286**, 33003–33011.

Hu, S., Jiang, W., Li, S., Song, W., Ji, L., Cai, L., et. al. (2015). Fucosylated chondroitin sulphate from sea cucumber reduces hepatic endoplasmic reticulum stress-associated inflammation in obesity mice. *Journal of Functional Foods*, **16**: 352-363.

Ilyas, A. A., Dalakas, M. C., Brady, R. O., & Quarles, R. H. (1986). Sulfated glucuronyl glycolipids reacting with anti-myelin-associated glycoprotein monoclonal antibodies including IgM paraproteins in neuropathy: Species distribution and partial characterization of epitopes. *Brain Research*, **385(1)**, 1–9.

Iozzo R. V. and Schaefer, L. (2015). Proteoglycan form and function: A comprehensive nomenclature of proteoglycans. *Matrix Biology*, **42**, 11-55.

Jaffer, U., Wade, R.G., Gourlay, T. (2010). Cytokines in the systemic inflammatory response syndrome: a review. *HSR Procedures in Intensively Care and Cardiovascular Anesthesia,* **2**: 161-175.

Kale, V., Freysdottir, J., Paulsen, B. S., FriÐjónsson, Ó. H., HreggviÐsson, G. Ó., & Omarsdottir, S. (2013). Sulphated polysaccharide from the sea cucumber *Cucumaria frondosa* affect maturation of human dendritic cells and their activation of allogeneic CD4(+) T cells *in vitro*. *Bioactive Carbohydrates & Dietary Fibre*, 2, 108–117.

Karamanou, K., Espinosa, D. C. R., Fortuna-Costa, A., Pavão, M. S. G. (2017). Biological function of unique sulfated glycosaminoglycans in primitive chordates. *Glycobiology Journal,* **34**: 277–283.

Kuschert, G. S., Coulin, F., Power, C. A., Proudfoot, A. E., Hubbard, R. E., Hoogewerf., et. al. (1999). Glycosaminoglycans interact selectively with chemokines and modulate receptor binding and cellular responses. *Biochemistry,* **38(39)**: 12959-12968.

Krichen, F., Bougatef, H., Sayari, N., Capitani, F., Ben Amor I., Koubaa, I., et. al. (2018). Isolation, Purification and Structural Characterestics of Chondroitin Sulfate from Smooth hound Cartilage: In vitro Anticoagulant and Antiproliferative Properties. *Carbohydrate Polymers* **197**, 451–459.

Krylov, V. B., Grachev, A. A., Ustyuzhanina, N. E., Ushakova, N. A. Preobrazhenskaya, M. E., Kozlova, N. I., et. al. (2011). Preliminary structural characterization, anti-inflammatory and anticoagulant activities of chondroitin sulfates from marine fish cartilage. Russian Chemical Bulletin, **60**, 746–753.

Lauder, R.M. (2009). Chondroitin sulphate: A complex molecule with potential impact on a wide range of biological systems. *Complementary Therapies in Medicine*, **17**, 56–62.

Lawrence, T. (2009). The Nuclear Factor NF-kB Pathway in Inflammation. *Cold Spring Harbor Perspectives in Biology*, **1**: a00165.

Lever, R., Mulloy, B., & Page, C. P. (2012). Ed. Heparin-a century of progress (Vol. **207**). Springer Science & Business Media.

Lima, M. A., Hughes, A. J., Veraldi, N., Rudd, T. R., Hussain, R., Brito, A. S., et al. (2013). Antithrombin stabilisation by sulfated carbohydrates correlates with anticoagulant activity. *Medicinal Chemistry Communication*, **4(5)**, 870–873.

Lopéz, M. L., Bruges, G., Crespo, G., Salazar, V., Deglesne, P. A., Schneider, H., et. al. (2014). Thrombin selectively induces transcription of genes in human monocytes involved in inflammation and wound healing. *Thrombosis Haemostasis*, **112**. 992-998.

Mosmann, T. (1983). Rapid colorimetric assay for cellular growth and survival: Application to proliferation and cytotoxicity assays. *Journal of Immunology Methods*, **65**: 55-63.

Mou, J., Li, Q., Qi, X. and Yang, j. (2018). Structural comparison, antioxidant and anti-inflammatory properties of fucosylated chondroitin sulfate of three edible sea cucumbers. *Carbohydrate Polymers*, **185**, 41–47.

Nadanaka, S., Kitagawa H., Sugahara K.. (1998). Demonstration of the immature glycosaminoglycan tetrasaccharide sequence GlcA-β1-3Galβ1-3Galβ1-4Xyl on recombinant soluble human α-thrombomodulin. A possible mechanism generating 'part-time' proteoglycan. *Journal of Biological Chemistry*, **273**, 33728–33734.

Nandini, C. D., Sugahara, K. (2006). Role of the Sulfation Pattern of Chondroitin Sulfate in its Biological Activities and in the Binding of Growth Factors. *Advances in Pharmacology*, **53**, 253-279.

Nakagawa N., Izumikawa T., Kitagawa H., Oka S. (2011). Sulfation of glucuronic acid in the linkage tetrasaccharide by HNK-1 sulfotransferase is an inhibitory signal for the expression of a chondroitin sulfate chain on thrombomodulin. *Biochemical and Biophysical. Research Communications*, **415**, 109–113.

Pavão, M. S. G., Vilela-Silva, A. C., Mourão, P. A.S. (2006). Biosynthesis of Chondroitin Sulfate: From the Early, Precursor Discoveries to Nowadays, Genetics Approaches. *Advances in Pharmacology*, **53,** 117-140.

Pomin, V. H., & Mourão, P. A. (2014). Specific sulfation and glycosylation - A structural combination for the anticoagulation of marine carbohydrates. *Frontiers in Cellular and Infection Microbiology*, **4**, 33.

Pomin V.H. (2015). A dilemma in the glycosaminoglycan-based therapy: synthetic or naturally unique molecules? *Medicinal Research Reviews*, **35**: 1195–1219.

Prabhakar, V., & Sasisekharan, R. (2006). The biosynthesis and catabolism of galactosaminoglycans. *Advances in Pharmacology*, **53**, 69-115.

Shetty, A. K. Kobayashi, T., Mizumoto, S., Narumi, M., Kudo, Y., Yamada, S. et. al. (2009). Isolation and characterization of a novel chondroitin sulfate from squid liver integument rich in N-acetylgalactosamine(4,6-disulfate) and glucuronate(3-sulfate) residues. *Carbohydrate Research*, **344(12)**, 1526-1532.

Smith, A. A. (2017). INFOS: spectrum fitting software for NMR analysis. *Journal Biomolecular NMR*, **67(2)**, 77-94.

Strande, J. L., and Phillips, S. A. (2009). Thrombin increases inflammatory cytokine and angiogenic growth factor secretion in human adipose cells *in vitro*. *Journal of Inflammation,* **6**:4.

Sugahara, K., Mikami, T., Uyama, T., Mizuguchi, S., Nomura, K., & Kitagawa, H. (2003). Recent advances in the structural biology of chondroitin sulfate and dermatan sulfate. *Current Opinion in Structural Biology*, **13(5)**, 612–620.

Sugahara, K., Tanaka, Y., Yamada, S., Seno, N., Kitagawa, H., Haslam, S. M., et al. (1996). Novel sulfated oligosaccharides containing 3-*O*-sulfated glucuronic acid from king crab cartilage chondroitin sulfate K. Unexpected degradation by chondroitinase ABC. *Journal of Biological Chemistry*, **271(43),** 26745–26754.

Tomatsu, S., Shimada, T., Patel, P., Mason, R. W., Mikami, T., Kitagawa, H., et al. (2015). Chondroitin and keratan sulfate. In M. Gama, H. B. Nader, & H. A. O. Rocha (Eds.). *Sulfated polysaccharides* (pp. 17–71). New York: Nova Science Pub Inc.

Ustyuzhanina, N.E., Bilan, M.I., Dmitrenok, A.S., Shashkov, A.S., Kusayakin, M.I., Stonik, V.A., Nifantiev, N.E., and Usov A.I., Structure and biological activity of a fucosylated chondroitin sulfate from the sea cucumber *Cucumaria japonica. Glycobiology* (2016) **26**, 449-459.

Ustyuzhanina, N. E., Bilan, M. I., Panina, E. G., Sanamyan, N. P., Dmitrenok, A. S., Tsvetkova, E. A. et. al. (2018). Structure and Anti-Inflammatory Activity of a New Unusual Fucosylated Chondroitin Sulfate from Cucumaria djakonovi. *Marine Drugs,* **16(10)**, 389.

Vranken W. F., Boucher W., Stevens T. J., Fogh R. H., Pajon A., Llinas M., et. al. (2005). The CCPN Data Model from NMR Spectroscopy: *Development of a Software Pipeline*, Proteins **59**, pp.687-696.

Volpi, N. (2006). Chondroitin sulfate: Structure, role and pharmacological activity Volume 53, 1st Edition. London: UK *Advances in Pharmacology*.

Volpi, N. (2011). Anti-inflammatory activity of chondroitin sulphate: new functions from an old natural macromolecule. *Inflammopharmacology,* **6**, 299–306.

Xu, L., Gao, N., Xiao, C. Lin, L. Purcell, S. W. Wu, M. et.al. (2018). Research paperModulating the degree of fucosylation of fucosylated chondroitinsulfate enhances heparin cofactor II-dependent thrombin inhibition. *European Journal of Medicinal Chemistry,* **154**, 133-143.

Zhang, T., Ma, Z., Wang, Y., Cheng, Z., et. al. (2010). Thrombin facilitates invasion of ovarian cancer along peritoneum by inducing monocyte differentiation toward tumor-associated macrophages-like cells. *Cancer Immunology, Immunotherapy*, **59(7)**: 1097-1108.

Zhu, W., Ji, Y., Wang, Y., He, D., Yan, Y., Su., et. al. (2018). Structural characterization and in vitro antioxidant activities of chondroitin sulfate purified from *Andrias davidianus* cartilage. *Carbohydrate Polymers*, **196**, 398–404.

Zigler, M., Kamiya, T., Brantley, E. C., Villares, G. J., Menashe Bar-Eli. (2011). PAR-1 and Thrombin: The Ties That Bind the Microenvironment to Melanoma Metastasis. *Cancer Research*, **71**(21):6561-6.